The song of the singing rod

Brian E. Anderson[a] and Wayne D. Peterson
Acoustics Research Group, Department of Physics and Astronomy, Brigham Young University, N283 ESC, Provo, Utah 84602

(Received 19 August 2010; revised 17 May 2011; accepted 28 September 2011)

This paper discusses basic and advanced aspects of the sound radiated by the singing rod demonstration commonly used in physics courses to depict an example of longitudinal waves. Various methods of exciting these rods are discussed along with the issues associated with each method. Analysis of the sound radiated by various rods with small-signal and large-signal excitations is presented for four different rods. The small-signal sound radiation consists of a fundamental frequency and odd harmonics (each corresponding to a longitudinal mode) when the rod is held at its midpoint. Large-signal sound radiation is highly dependent on the rod's geometry. The large-signal sound can possess strong even harmonics and/or beating tones resulting from modal coupling of transverse bending modes and either subharmonic longitudinal modes or torsional modes. A detailed analysis of the sound radiation from a singing rod can provide excellent laboratory exercises or classroom demonstrations for advanced undergraduate or graduate level acoustics courses whose scope includes resonances of a bar. © *2012 Acoustical Society of America*.
[DOI: 10.1121/1.3677249]

PACS number(s): 43.10.Sv, 43.40.Cw, 43.40.Ga [VWS] Pages: 2435–2443

I. INTRODUCTION

In elementary physics courses it is common to utilize the so-called singing rod demonstration to illustrate the concept of longitudinal wave resonances in solid media. One holds a long metal rod (usually aluminum) between two fingers at the midpoint of the rod's length. Two fingers on the other hand are then used to rub the rod longitudinally in a steady motion. The key to excitation of the longitudinal modes is the use of a substance to create sufficient friction between the fingers and the rod. Through tactile inspection of one end of the rod, one may observe longitudinal motion by noting that the motion along the axis of the rod is greater than the motion perpendicular to the rod's axis.

To the authors' knowledge, the first citation, albeit brief, of the idea of the singing rod demonstration was by Meiners.[1] Naba[2] and Nicklin[3] then suggested ideas for obtaining the frequencies of resonance of the singing rod in a classroom or laboratory setting. Rossing and Russell[4] provided an excellent review of longitudinal, torsional, and bending wave modes in a bar. They also described a means to observe a rod's modal frequencies in steady state with an electromagnetic excitation for a laboratory experiment. Later at a sectional American Physical Society meeting, Minnix *et al.*[5] presented the idea that singing rods driven with sufficient amplitudes "scream" intermittently when the rod vibration couples with a transverse mode, although this work was never written up. Errede[6] wrote an unpublished report on the physics of the singing rod and suggested a means to rotate the rod after exciting it to create a Doppler shift beating effect in the classroom. Finally, Machorro and Samano[7] presented a laboratory exercise to measure the speed of sound in a singing rod by determining the angles where interference minima occur in the radiation patterns, considering the ends of the singing rod as two in-phase sources.

The purpose of this paper is to characterize the sound radiation from a few different aluminum rods (singing rods). Various methods to excite a singing rod are described. Observations of the excitation phase and the decay phase of the sound radiation are made. Calibrated sound pressure levels of the typical sound radiation from the singing rods are presented. The difference between the small-signal and large-signal excitations of the singing rods are explained, yielding further teaching opportunities in a classroom or laboratory exercise. The large-signal, sound radiation may contain tones resulting from bending modes, torsional modes, and subharmonic longitudinal modes, and sometimes a beating effect when two of these modes are in close proximity. Recently, Krueger *et al.* showed that beating tones can arise from nonlinear modal coupling in the structural vibration and can result in highly desirable tonal quality of gongs in some cultures.[8] It is postulated here that the apparent nonlinear behavior of singing rods of certain geometries is due to a similar nonlinear modal coupling as the rod vibrates with sufficient amplitude.

II. BACKGROUND

Theoretical derivations of the longitudinal, torsional, and bending modes for a homogeneous rod are given by many (see, e.g., Ref. 4). As a review, this section will give expressions for the frequencies of resonance for each of these types of modes.

A. Longitudinal modes

The frequencies of resonance for longitudinal modes of a constant cross section, free–free rod (regardless of whether

[a]Author to whom correspondence should be addressed. Electronic mail: bea@byu.edu

the rod is solid or hollow, or whether the cross section is rectangular or cylindrical) are harmonically related so that

$$f_L = \frac{n}{2L}\sqrt{\frac{E}{\rho}}, \qquad n = 1, 2, 3, ..., \tag{1}$$

where n is the mode number, L is the length of the rod, E is the Young's modulus of elasticity of the rod, and ρ is the mass density of the rod. The nodes $\xi_m(x)$ of the rod for a given mode n are located at

$$\xi_m(x) = \frac{mL}{n+1}, \qquad m = 1, 2, 3, ..., n. \tag{2}$$

B. Torsional modes

The frequencies of resonance for torsional modes of a free–free cylindrical rod are also harmonic, such that

$$f_T = \frac{n}{2L}\sqrt{\frac{E}{2\rho(1+\sigma)}}, \qquad n = 1, 2, 3, ..., \tag{3}$$

where σ is Poisson's ratio. The torsional wave speed for rods of noncircular cross sections is somewhat lower due to a decrease in the radii of gyration (the radius of gyration is essentially the average radius of an object's parts, as it bends, from its center of gravity). The resonance frequencies for a square rod are 0.92 times the expression given in Eq. (3).[4] For a rectangular rod, with the width twice the thickness, the frequencies are 0.74 times the expression in Eq. (3).[4] The nodes of these torsional modes are located at the same locations as those for longitudinal modes [see Eq. (2)].

C. Bending modes

The frequencies of resonance for bending modes of a free–free rod are not harmonically related due to the dispersive nature of the bending wave speed. The bending wave speed of a rod depends on the radius of gyration, κ, of the rod (determined by its cross-sectional geometry). These resonance frequencies are given by Kinsler *et al.*[9]

$$f_B = \left(3.011^2, 5^2, 7^2, 9^2, ...\right)\frac{\pi\kappa}{8L^2}\sqrt{\frac{E}{\rho}}. \tag{4}$$

Note the difference in the dependence on the length for f_B versus the dependence for f_L and f_T. Thus f_B are more sensitive to changes in length. For a solid cylindrical rod, $\kappa = a/2$, where a is the radius.[10] For a hollow cylindrical rod, $\kappa = \sqrt{a^2 + a_i^2}/2$, where a_i is the inner radius.[10] For a solid rectangular rod, $\kappa = h/\sqrt{12}$, where h is the rod thickness.[10] For a hollow rectangular rod, $\kappa = \sqrt{\left(bh^3 - b_i h_i^3\right)/[12(bh - b_i h_i)]}$, where b is the width (where, in general, $L > b > h$), b_i is the inner width, and h_i is the inner thickness of the rod.[10] The previous analysis is based upon the Bernoulli–Euler theory and therefore neglects the effects of shear deformation and rotary inertia. The Timoshenko theory, an improvement upon the Bernoulli–Euler theory, incorporates these effects and results in a decreased sound speed with increasing frequency relative to the predicted Bernoulli–Euler wave speed. Thus, we expect the predicted bending wave modal frequencies to be somewhat higher than measured values, and for this departure to be more significant for higher numbered modal frequencies. Similar findings were reported by Rossing and Russell.[4]

D. Common nodes

As stated previously, the torsional modes have nodes in the same locations as the longitudinal modes.[7] If the rod is firmly held at the midpoint along its length then only the odd-numbered modes of each of these types of modes should possibly be excited, as they all possess a common node at the midpoint (noting that longitudinal motion would induce some transverse component due to the Poisson effect[11]). The bending wave mode nodal locations are more complicated to determine, but all of the even-numbered modes have a node at the midpoint, whereas all of the odd-numbered modes have an antinode at the midpoint.[9] Thus, it is conceivable that when a singing rod is held at its midpoint and subsequently excited, the radiated sound will primarily contain contributions from the odd-numbered longitudinal modes and torsional modes and from the even-numbered bending modes.

III. ROD EXCITATION

A. Methods of excitation

To excite longitudinal modes in a singing rod, it is ideal to support the rod with two fingers of one hand and slide two fingers of the opposite hand along one end of the rod. Typically one places the thumb and either index finger or middle finger opposite each other at the middle of the length of the rod to induce a vibration node. One then uses a similar combination of fingers of the opposite hand to slide along one end of the rod as depicted in Fig. 1. A steady velocity and

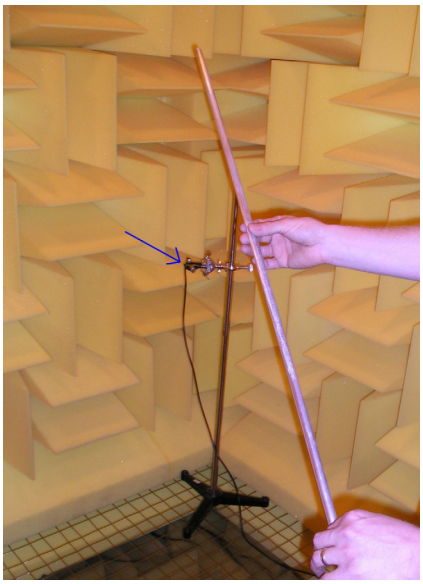

FIG. 1. (Color online) Photograph of a singing rod being played in the anechoic chamber. The microphone is identified by the arrow.

constant applied force with the sliding hand's fingers excites a rod into longitudinal resonance. A shrill pitch from a singing rod will wake up any classroom. Repeated excitation by the sliding hand as the rod is singing allows excitation of successively higher vibration amplitudes. Because the rod is gripped at the center, only the fundamental longitudinal mode and odd harmonics are expected to be excited. One can then place their node hand at different nodal positions of higher longitudinal modes to excite higher order longitudinal modes of the rod (including exciting the higher harmonics that have matching nodal positions).

Traditionally it has been suggested that violin rosin be applied lightly to the finger tips of the sliding hand. The downside of using rosin is the residue that it leaves on the fingers. We have found one may avoid application of rosin or another powder directly to the fingers if Octadecanol (also known as stearyl alcohol or octadecyl alcohol) powder, of molecular weight 270, is applied to the rod. This powder sticks to the rod and remains for a long time. The advantage of the powder is that the residue is colorless and a minimal amount remains on the fingertips.

Other excitation methods may be used. Powder-free nitrile gloves may also be used to excite a rod. The thickness of the glove material influences the ease of excitation. For example 0.004 in. thick nitrile gloves are easier to use to excite an aluminum rod than 0.0055 in. thick nitrile gloves. We have also found that spraying methyl alcohol onto a paper towel and sliding the paper towel on the rod also excites the rod. Neither a paper towel wet with water excite the rod, nor the methyl alcohol paper towel once it dries somewhat. Apparently the wet methyl alcohol's evaporation at room temperature creates a friction mechanism.

B. Measurements of excitation

In order to determine the interaction between the sliding fingers and the rod, accelerometers are affixed onto the fingernail of the sliding hand thumb (ST) and to the fingernail of the node hand thumb (NT) using bees wax. Accelerometers placed on an end of the rod causes the vibrations to damp out too quickly. The use of a laser vibrometer would be ideal but it is difficult to hold the rod steady enough for the laser to acquire data. Clamping the midpoint was found to be very challenging, either resulting in damping out the vibrations too quickly or clamping too much of the length of the rod at the midpoint. Thus, we determined that accelerometers mounted on thumbs were a decent method to monitor the rod vibration. The accelerometers are axial and thus respond to vibration perpendicular to the rod's long axis. As the sliding hand excites the rod, the acceleration is measured.

Figure 2(a) displays a few cycles of the acceleration waveform from the ST accelerometer. Note the triangle wave shape of the waveform, indicative of a stick-slip interaction that is common with the playing of bowed string instruments (a driven string).[12] However, the stick times and the slip times vary as the rod is excited (as the point of excitation is changing and the amplitude is increasing), whereas in musical instruments these times remain fairly consistent (where the point of excitation does not change in general). The waveform is sawtooth in nature, meaning that a fundamental frequency and all harmonics (even and odd) are likely present. Figure 2(b) displays the waveform as recorded by an accelerometer mounted onto the NT, located at the midpoint of the rod. One can see the rise in energy up to $\sim$1.45 s as the sliding hand excites the rod, constituting

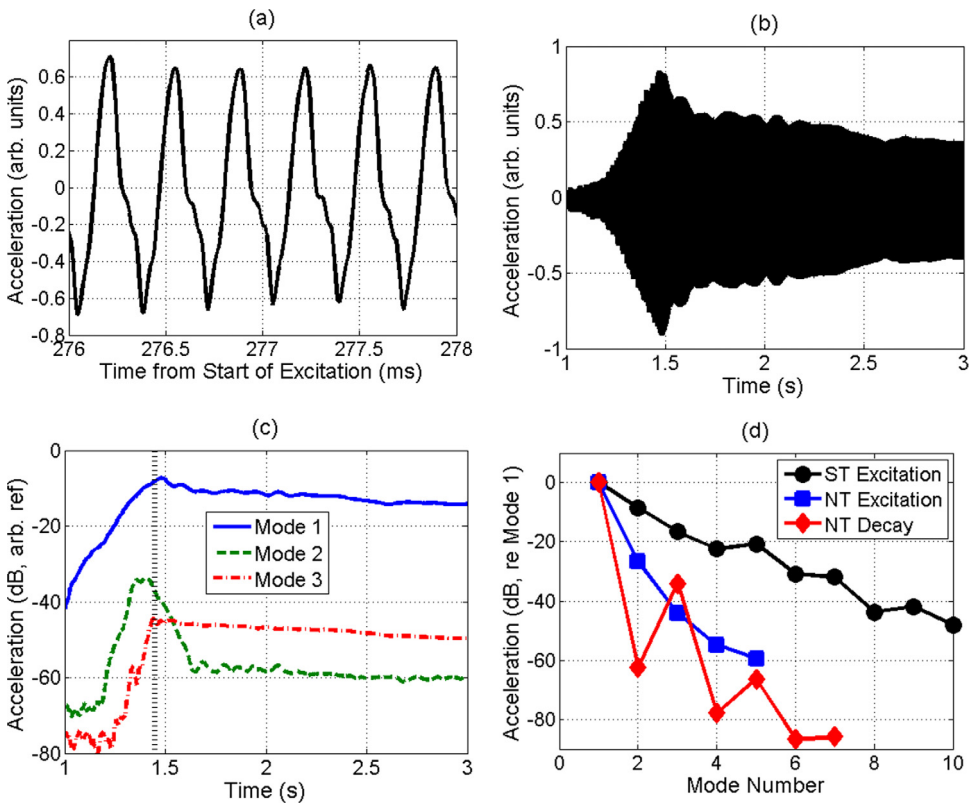

FIG. 2. (Color online) Example excitation and decay of the vibration of a singing rod measured with accelerometers. (a) A few sample cycles of the waveform measured with the accelerometer mounted onto the sliding thumb, illustrating the stick-slip excitation. (b) Measured acceleration waveform from the accelerometer mounted onto the node thumb. (c) Instantaneous acceleration amplitudes measured with the node thumb accelerometer for the first three longitudinal modes of a singing rod (the dotted vertical line indicates the transition between the excitation and decay portions of the signal). (d) Acceleration amplitudes measured with the sliding thumb (ST) and node thumb (NT) accelerometers for various longitudinal modes during excitation and decay (ST decay is not applicable as the ST leaves the rod after excitation).

the excitation phase. At ~1.45 s the sliding hand releases the rod and the acceleration then decreases during the decay phase. In Fig. 2(c), the instantaneous acceleration amplitude (determined through application of appropriate narrow bandpass filters) of each of the first three modes, as recorded by the NT accelerometer, is displayed. During the excitation phase each of the first three modes are excited (along with other higher order modes, although only the first three are displayed). The theory developed in Sec. II suggested that the even-numbered longitudinal modes should not be easily excited because they possess antinodes at the midpoint of the rod. As soon as the sliding hand leaves the rod the second mode's acceleration quickly drops 25 dB, whereas the first and third modes decay less rapidly. The rapid decay of the second mode is due to the damping induced by the node hand being located at one of the antinodes for the second mode. Figure 2(d) shows the relative acceleration amplitudes of various modes, taken from normalized Fourier transforms during the duration of each respective phase, during the excitation of the rod (from the ST accelerometer) and the decay of the rod's vibration (from the NT accelerometer). Note the fairly constant amplitude rolloff with increasing mode number during the excitation, for both the ST and NT accelerometers), suggesting that the node hand is not significantly affecting the excitation of even-numbered modes. In contrast, note the relative higher amplitudes of the odd-numbered modes compared to the even-numbered modes during the decay phase, confirming that the node hand damps out the even-numbered modes as expected. This analysis suggests that the timbre of the sound changes between the excitation phase and the decay phase due to the differences in harmonic content.

IV. MEASUREMENTS

The analysis presented in Sec. III B discusses the longitudinal modes that are present during the excitation and decay phases of singing rod excitation when the rod is excited at relatively low amplitudes. Here we will show that even-numbered bending modes, odd-numbered torsional modes, and subharmonic longitudinal modes, along with coupling between these modes, can also be excited during the decay phase when the rod is excited with a larger amplitude, suggesting nonlinear behavior. The rod is excited with larger amplitude by increasing the force applied by the sliding hand fingers and/or by exciting the rod multiple times with the sliding hand. There is an apparent abrupt amplitude threshold, below which the small signal sound is heard and above which the large signal sound is also heard. The nonlinearity does not appear to be an acoustic nonlinearity generated in the air, but rather within the large vibrations in the rod.

Each of the experiments presented in this section were performed in an anechoic chamber with working dimensions $3.00 \times 2.38 \times 2.59$ m. This anechoic chamber has a low frequency cutoff limit of 125 Hz. The radiated sound was recorded with a 12.7 mm (1/2 in.) type-1 precision ICP® condenser microphone placed ~0.5 m away from the one end of each rod. The rod was held at an angle of ~30° from horizontal. Octadecanol powder is rubbed onto one end of each of the rods. Figure 1 displays a photograph of the rod being excited in the anechoic chamber with the microphone identified by the arrow. A sampling frequency of 96 kHz was used in the microphone recordings. Each calibrated spectrogram shown in this section utilizes 3000 point segments, a Hamming window, and 50% overlap of time segments.

Each of the rods is ~182.88 cm (6 ft) in length, although the actual lengths vary slightly and are denoted below. The rods are 6061 aluminum with material properties of $E = 68.9$ GPa, $\rho = 2700$ kg/m^3, and $\sigma = 0.33$. A rod of this length would have a longitudinal mode fundamental frequency of 1381 Hz. The torsional and bending mode frequencies depend on the radius of gyration of the rod and therefore the respective cross-sectional geometry of the rod. The predicted longitudinal modal frequencies for each of the four rods studied in this paper, based on Eq. (1) are tabulated in Table I. Table II gives the predicted torsional mode frequencies for each rod based on Eq. (3), and Table III gives the predicted bending mode frequencies based on Eq. (4).

A. Hollow rectangular rod

The first singing rod, whose small- and large-signal behavior is examined, is a hollow rectangular rod. The outer cross-sectional dimensions of the rod are 3.81×1.91 cm ($1.5 \times 3/4$ in.). The walls of the rod are 0.318 cm thick (1/8 in.) and the rod is 182.80 cm in length. Figure 3(a) displays a sample spectrogram of the sound radiated by the rod with a small-signal excitation, as recorded by the microphone. Note that the first, third, and fifth modes (at 1390, 4170, and 6950 Hz, respectively) are more prominent than the second and fourth modes (at 2780 and 5560 Hz, respectively) as expected.

Figure 3(b) displays a sample spectrogram of the sound radiated by the rod with a large-signal excitation, as recorded by the microphone. The rod was excited multiple times to achieve the large-signal behavior whose decay phase starts at ~2.7 s. One observes that from 2.5 to 2.7 s modes 1–7 are all briefly excited during the excitation phase. After the excitation phase has ended there is a strong apparent subharmonic at 695 Hz corresponding to half the frequency of the first mode. Additional new content at 2085 and 3475 Hz is also observed, each corresponding to 3/2 and 5/2 times the fundamental mode frequency, respectively. The subharmonic at 695 Hz is likely evidence of nonlinear wave

TABLE I. Predicted longitudinal mode frequencies (rounded to the nearest hertz) for the four singing rods in this study.

	Rectangular		Cylindrical	
Mode number	Hollow	Solid	Hollow	Solid
1/2[a]	691	690	693	693
1	1382	1380	1387	1387
2	2763	2760	2773	2773
3	4145	4140	4160	4160
4	5527	5520	5546	5546
5	6909	6900	6933	6933

[a]The 1/2 mode number corresponds to the subharmonic frequency.

TABLE II. Predicted torsional mode frequencies (rounded to the nearest hertz) for the four singing rods in this study.

	Rectangular		Cylindrical	
Mode number	Hollow	Solid	Hollow	Solid
1	627	778	850	850
2	1254	1557	1700	1700
3	1881	2335	2550	2550
4	2508	3114	3401	3401
5	3135	3892	4251	4251

behavior in the rod. Others have observed subharmonic generation in many types of acoustic and vibration systems (see a nice review of early work in Ref. 13), including work showing subharmonics in cymbal musical instruments.[14–17] Apparently it is common for subharmonics to have a certain amplitude threshold before they appear[18] and this is indeed the case for the singing rods examined here. The acoustic sound pressure levels generated by the singing rods in the current study are not sufficient to induce nonlinear wave steepening in the air, rather the authors believe that the nonlinearity is generated in the structural vibrations within the rod.

There is an apparent beating effect visible in the spectrogram of Fig. 3(c) at 695 Hz after 2.7 s and it is quite audible with a beat frequency of 5.5 Hz. This figure is zoomed in and its amplitude color scale is adjusted to clearly show the beating in the spectrogram. The beating shows up as amplitude fluctuations in the spectrogram. The beating of the subharmonic frequency calls for further analysis. The sixth bending mode for this rod would be 718 Hz. Rossing and Russell[4] found that the measured bending mode frequencies fell slightly below the predicted frequencies with the Bernoulli–Euler theory as expected, as shear deformation and rotary inertia are neglected. They also found that at a

TABLE III. Predicted bending mode frequencies (rounded to the nearest hertz) for the four singing rods in this study.

	Rectangular		Cylindrical	
Mode number	Hollow	Solid	Hollow	Solid
1	39	20	22	17
2	106	54	59	48
3	208	106	116	93
4	344	176	192	154
5	514	263	287	230
6	718	367	401	321
7	956	488	534	427
8	1228	627	686	549
9	1534	784	857	685
10	1874	957	1046	837
11	2248	1148	1255	1004
12	2656	1357	1483	1186
13	3098	1583	1730	1384
14	3574	1826	1995	1596
15	4084	2086	2280	1824
16	4628	2364	2584	2067
17	5206	2659	2906	2325
18	5818	2972	3248	2598

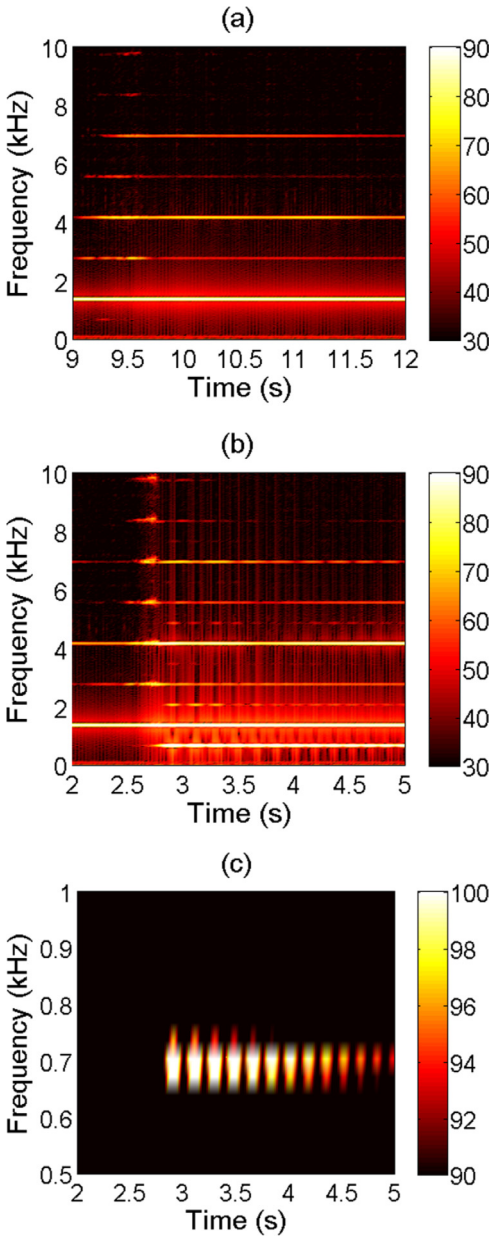

FIG. 3. (Color online) Example spectrograms of small-signal and large-signal excitations of a 3.81 cm × 1.91 cm × 182.80 cm hollow rectangular singing rod (0.318 cm wall thickness) in (a) and (b), respectively, measured by a microphone. Amplitude is represented in calibrated sound pressure level (dB re 20 μPa). (c) Zoomed-in display of the data in (b) with a different amplitude color scale.

frequency midway between a torsional mode and a bending mode that they could "observe motion which combines these two normal modes." It is postulated here that the beat frequency effect found in Fig. 3(c) is due to a similar coupling, as found by Rossing and Russell, although of the subharmonic longitudinal mode and the sixth bending mode (their rod had quite a different geometry than the present one).

An analysis (not presented here), employing the so-called instantaneous frequency method,[19–24] of the beat frequency reveals that it slightly increases over time as the rod vibration decays. One can audibly hear the increase in the beat frequency as well (increase of 1–2 Hz). This may be due to slight shifts in resonance frequencies as the length of the rod dynamically changes with large excitation amplitude.

During dynamic vibration the bending wave mode frequencies would be affected more by length changes than longitudinal mode frequencies due to their relative dependencies on rod length [see Eqs. (1) and (4)]. Further research could be done to verify this.

B. Solid rectangular rod

A solid square rod of thickness 1.27 cm (1/2 in.) and length 183.04 cm is now analyzed. This rod is excited multiple times and with a significant amount of force applied by the sliding hand and there is not a noticeable difference in the sound quality of the rod with larger excitation. Figure 4 displays a sample spectrogram as recorded by the microphone. Note the strong fundamental frequency at 1359 Hz and its odd harmonics. In this experiment, the rod is initially excited and set into its decay phase at ~ 1.0 s. Note the generation of all harmonics during the excitation phase roughly from 0.5 to 1 s. It is then excited a second time at $\sim$3.2 s, again confirming the findings from Sec. III B. that all harmonics are excited during the excitation phase.

When the rod is excited a second time (from 3.2 s on), one can observe that the even harmonics remain in the decay phase, albeit at lower amplitudes than their neighboring odd harmonics. The amplitude of the second harmonic during the second excitation is 30 dB higher than in the first excitation, whereas the amplitudes of the first and third harmonics rise only 14 dB in the second excitation compared to the first (similar findings can be made for other even and odd harmonic amplitudes). Thus, the generation of the even harmonics in the second excitation appears to suggest that the second excitation is of sufficient amplitude to generate nonlinearity in the vibration, as the added energy is unevenly distributed among the mode frequencies.

C. Hollow cylindrical rod

We now analyze cylindrical rods and begin with a hollow cylindrical rod of diameter 1.27 cm (1/2 in.), length 182.17 cm, and wall thickness 0.159 cm (1/16 in.). The hollow cylindrical rod is the easiest rod to excite in terms of the applied force necessary by the sliding hand. Figure 5(a) displays a sample spectrogram of a microphone recording of its

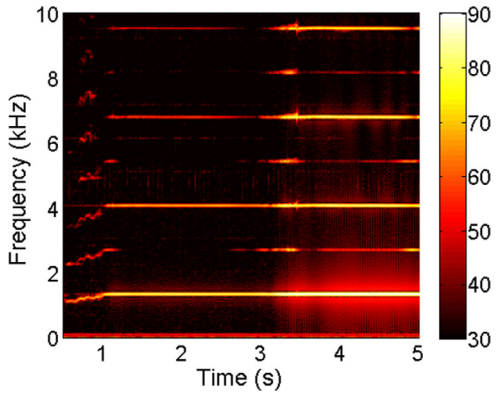

FIG. 4. (Color online) Spectrogram of the large-signal excitation of a 1.27 cm × 1.27 cm × 183.04 cm solid rectangular singing rod. Amplitude is represented in calibrated sound pressure level (dB re 20 μPa).

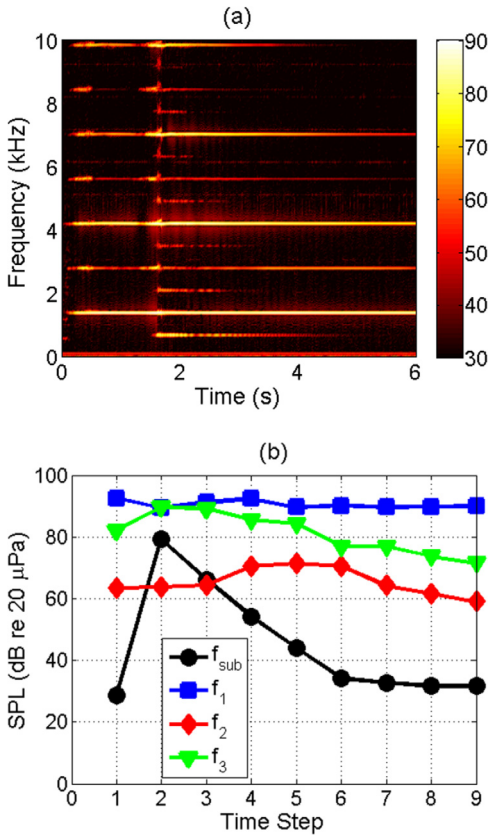

FIG. 5. (Color online) (a) Spectrogram of the large-signal excitation of a 1.27 cm diameter, 182.17 cm long hollow cylindrical singing rod (0.159 cm wall thickness). Amplitude is represented in calibrated sound pressure level (dB re 20 μPa). (b) Amplitudes at various time segments (steps) for the subharmonic, first, second, and third longitudinal modes.

sound. The figure depicts a first excitation between 0.1 and 1.5 s and a second excitation from 1.5 s on. Note that even with a lower level excitation (the first excitation) the even harmonics are present, although again at lower amplitudes relative to the odd harmonics. It is also apparent from Fig. 5(a) that during the second excitation that a subharmonic and higher integer multiples of the subharmonic, are generated. A beating effect also takes place likely between the subharmonic at 702 Hz and the eighth bending mode at 686 Hz. Each of these effects are similar in nature to the sound radiated by the hollow rectangular rod.

Figure 5(b) displays the amplitude of various harmonic components versus different time segments (or steps). Each time step is 0.83 s in duration. The first time step is taken from the middle of the first excitation (between 0.42 and 1.25 s). The subsequent time steps, 2–9, are taken between 1.56 and 8.23 s [not all shown in Fig. 5(a)] with no overlap. The noise floor is $\sim$30 dB for the modal frequencies displayed. Note the lack of the subharmonic for the first excitation (it is in the noise floor). The subharmonic is then excited in the second excitation and it decays more rapidly than the first three harmonics. It is interesting to note that the levels of the harmonics are not much different between the first excitation and the first segment of the second excitation for the first and third harmonics. Thus, when the rod is excited the second time, the vast majority of the added energy results in the excitation of the subharmonic, again suggesting a nonlinear effect

as the energy at the fundamental frequency did not rise with increasing input energy.

D. Solid cylindrical rod

Finally we analyze the sound radiated by a solid cylindrical rod of diameter 1.27 cm (1/2 in.), and length 182.17 cm. These are the same outer dimensions as for the hollow cylindrical rod. Figure 6 displays a sample spectrogram of a microphone recording of its sound. During this recording, the rod is set into its first decay phase at 0.5 s. A second excitation takes place just after 2.0 s.

Note that nearly a half-second after the first excitation, two tones appear at 543 and 827 Hz. These two tones are not subharmonically related to the fundamental frequency. However, the predicted eighth and tenth bending mode frequencies for this rod are at 549 and 837 Hz, respectively, suggesting that these two modes are responsible for these two tones. A beating effect is apparent at the 827 Hz tone (that is quite audible). The first predicted torsional mode of this rod occurs at 850 Hz and it is likely that the beating results from a similar effect, as observed by Rossing and Russell,[4] noted in Sec. IV A.

When this first rod is excited the second time, the 543 and 827 Hz tones remain. Additionally, tones at 1168, 1570, and at 2540 Hz are generated. These additional tones likely result from the 12th, 14th, and 18th bending modes as the predicted modal frequencies are at 1186, 1596, and at 2598 Hz, respectively. Although not as apparent from the spectrograms, the third longitudinal mode at 4110 Hz peaks at 104 dB and it nearly dominates the audible radiated sound.

This particular rod is actually difficult to excite without exciting the 837 Hz tone, although it is possible. The measured level of the fundamental frequency with a small-signal excitation just below the apparent threshold of generating the 837 Hz tone is 80 dB. In contrast, the level at the fundamental frequency is 89 dB for the first excitation, displayed in Fig. 6, and 91 dB for the second excitation.

A second rod of the same geometry (exact same length) is found to exhibit the same beating effect as observed between the first torsional mode and the tenth bending mode. In an effort to shift the bending mode frequency away from the torsional mode frequency, this second rod is then cut down by 12.7 cm (5 in.) to shift the tenth bending mode frequency to 967 Hz and the first torsional mode frequency to 914 Hz. The shorter length increases all predicted longitudinal and torsional mode frequencies by 7.5%, whereas the predicted bending mode frequencies are increased by 15.5%. After the rod is cut the beating effect can no longer be excited even with significantly large excitation amplitudes as the torsional and bending mode frequencies are no longer in close proximity.

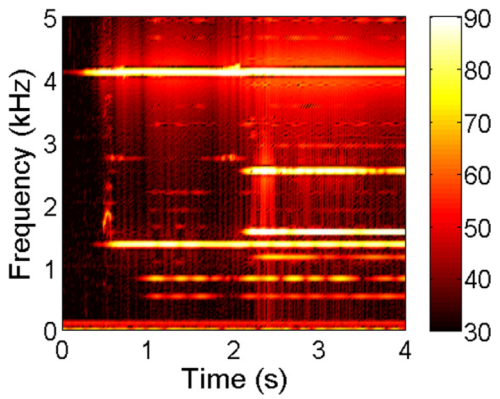

FIG. 6. (Color online) Spectrogram of the large-signal excitation of a 1.27 cm diameter, 182.17 cm long solid cylindrical singing rod. Amplitude is represented in calibrated sound pressure level (dB re 20 μPa).

V. EDUCATIONAL CONSIDERATIONS

The singing rod demonstration is well known and has been used for many years by physics educators as an example of the existence of longitudinal wave motion. Educators commonly show that the location of the node hand determines which longitudinal mode numbers radiate. Additionally, they also show that rods of different cross section geometries (solid versus hollow, or rectangular versus cylindrical), but of the same length, may be used to show that longitudinal modes of a rod only depend on the rod's length. In this paper, we have presented complex nonlinear phenomena in singing rods that may be used to illustrate advanced topics in acoustics and vibration. The purpose of this section is to provide some ideas for advanced demonstrations with singing rods. It is recommended that an educator have a running spectrogram (several free programs are available online) displayed in the classroom as the rods are excited so that the educator can discuss the various frequencies generated.

In this paper we have shown that one may design a singing rod's geometry such that bending modes and torsional modes may also be predicted and observed. These modes are enabled when the length of the rod is adjusted such that a predicted even-numbered bending mode frequency nearly matches the modal frequency of either a subharmonic longitudinal mode or of a torsional mode. It appears from our experiments that unless this near matching of modal frequencies occurs, torsional and bending modes cannot be observed.

The importance of the vibrational pattern of the rod, in terms of the locations of nodes and antinodes, can also be illustrated as two rods of the same cross-sectional geometry but of different lengths can be designed to more easily exhibit nonlinear coupling of a bending mode with either a subharmonic longitudinal mode or with a torsional mode. One rod may be cut to a length to potentially enable the nonlinear coupling of the subharmonic longitudinal mode and an *even*-numbered bending mode, whereas a second rod is cut to a length to potentially enable the nonlinear coupling of the subharmonic longitudinal mode and an *odd*-numbered bending mode. Only the rod tuned to the even-numbered bending mode will exhibit the nonlinear beating as it shares a node at the rod's midpoint, and therefore radiates more efficiently. To determine the ideal length, L_{L-B}, to enable coupling of the subharmonic longitudinal mode with an even numbered bending mode, Eq. (1) with $n = 1/2$ is set equal to Eq. (4) including only the even modes and solving for L, resulting in

$$L_{L-B} = \frac{\pi}{2}\kappa(2n+1)^2, \qquad n = 2, 4, 6, \ldots. \tag{5}$$

The ideal length, L_{T-B}, to enable coupling of the first torsional mode with an even numbered bending mode is found by setting Eq. (3) with $n = 1$ equal to Eq. (4) including only the even modes and solving for L, resulting in

$$L_{T-B} = \frac{\pi\kappa}{4\sqrt{2(1+\sigma)}}(2n+1)^2, \qquad n = 2, 4, 6, ... \quad (6)$$

In each of these two length calculations, it should be remembered that Eq. (4) is based on the Bernoulli–Euler theory and those bending mode frequencies should be slightly higher than that found experimentally. Thus, the educator should consider trimming off some of the lengths given in Eqs. (5) and (6) to achieve the best coupling.

The spacing of the modal frequencies for the various types of modes may be used to illustrate the concept of dispersion (a medium with a frequency-dependent wave speed). In the case of longitudinal and torsional waves, which possess frequency-independent wave speeds, the higher order modal frequencies are integer multiples of the fundamental frequency and therefore longitudinal and torsional waves are not dispersive. On the contrary, bending waves possess a frequency-dependent wave speed and thus their higher order modal frequencies are not harmonics of the fundamental frequency, which is evidence of dispersion. If the instructor designs a rod such that many bending modes are excited, they can then display the spectrum of the singing rod's modal frequencies and point out the lack of integer multiple spacing of its harmonics.

VI. CONCLUSIONS

The song of the singing rod can be quite complex. All harmonics are present as the rod is excited, even for small signal excitation. After small signal excitation, the even-numbered modes decay out, when the rod is held at its midpoint. For a singing rod of a given geometry, there is an apparent threshold when the large-signal, nonlinear behavior of the rod comes into play (the threshold depends on the rod's geometry). The large-signal radiated sound contains tones due to bending modes, torsional modes, subharmonic longitudinal modes, and increased radiation of the even-numbered longitudinal modes (the reason for the increased radiation efficiency of even-numbered modes is not known). It is also possible for the large-signal radiated sound to exhibit a beating effect possibly due to nonlinear modal interaction.

It is generally easier to excite hollow rods at larger amplitudes than solid rods. From an education standpoint, the radiated sound from solid rods may provide more interesting spectra, due to the rich harmonic content and nonlinear modal coupling (if their lengths are such that coupling exists between bending and torsional modes).

Measurements made by placing accelerometers on the thumbs of someone exciting a singing rod, at small amplitudes, show that all longitudinal modes are present during the stick-slip excitation of the rod. When the sliding hand leaves the rod the even-numbered modes tend to decay rapidly and the sound is dominated by the odd harmonics (only for small-signal excitation). Various means to create the friction necessary to excite an aluminum rod were discussed. We recommend the use of Octadecanol powder with a molecular weight of ~270, due to the ease of rod excitation, no need to apply any substance to the fingers, and the lack of residue remaining on the fingers after excitation of the rod (except during the initial application of Octadecanol onto the rod).

The large-signal radiated sound is highly dependent on the rod's geometry. The threshold for additional tonal generation is dependent on the rod's geometry, e.g., when the proximity of an even-numbered bending mode frequency to the subharmonic of the fundamental longitudinal mode frequency is small. A beating effect can also occur when the frequency difference between these mode combinations (even-numbered bending mode and subharmonic longitudinal mode) is small. It is apparent that the subharmonic tone is not excited unless its frequency is close to that of an even-numbered bending mode frequency.

Advanced demonstration ideas have been presented to allow educators to predict and observe torsional and bending modes, illustrate the concept of dispersion, and illustrate the importance of the locations of nodes and antinodes (with application to musical instruments for example).

ACKNOWLEDGMENTS

The authors thank Samuel Anderson and Brad Solomon for assistance in conducting preliminary experiments for a laboratory assignment as part of their coursework for a graduate level acoustics course. The authors also thank John Ellsworth for machining assistance and Kent Gee for helpful comments and insights.

[1]H. F. Meiners, *Physics Demonstration Experiments* (Ronald, New York, 1970), Vol. I, p. 496.
[2]N. Naba, "Observation of longitudinal vibration of metal rods," Am. J. Phys. **40**(9), 1339–1340 (1972).
[3]R. C. Nicklin, "Measuring the velocity of sound in a metal rod," Am. J. Phys. **41**(5), 734–735 (1973).
[4]T. D. Rossing and D. A. Russell, "Laboratory observation of elastic waves in solids," Am. J. Phys. **58**(12), 1153–1162 (1990).
[5]R. B. Minnix, D. R. Carpenter, and W. W. McNairy, "How to make singing rods scream," 66th Annual Meeting of the Southeastern Section of the American Physical Society (November 7–9, 1999).
[6]S. Errede, "The physics of a longitudinally vibrating singing metal rod," see http://online.physics.uiuc.edu/courses/phys498pom/Lecture_ Notes/Vibrating_Rod/Longitudinally_Vibrating_Singing_Rod.pdf (Last viewed August 19, 2010).
[7]R. Machorro and E. C. Samano, "How does it sound? Young interferometry using sound waves," The Phys. Teacher **46**, 410–412 (2008).
[8]D. W. Krueger, K. L. Gee, and J. Grimshaw, "Acoustical and vibrometry analysis of a large Balinese gamelan gong," J. Acoust. Soc. Am. **128**(1), EL8–EL13 (2010).
[9]L. E. Kinsler, A. R. Frey, A. B. Coppens, and J. V. Sanders, *Fundamentals of Acoustics*, 4th ed. (Wiley, New York, 2000), pp. 68–87.
[10]J. M. Lessells, G. S. Cherniak, and J. E. Love, Jr., "Mechanics of deformable bodies," in *Handbook of Engineering Fundamentals*, 3rd ed., edited by O. W. Eshbach (Wiley, New York, 1975), pp. 513–514.
[11]L. D. Landau and E. M. Lifshitz, *Theory of Elasticity*, 3rd ed. (Elsevier, Oxford, UK, 1986), p. 12.
[12]W. J. Strong and G. R. Plitnik, *Music Speech Audio*, 3rd ed. (BYU Academic, Provo, UT, 2007), pp. 375–384.
[13]N.-C. Yen, "Subharmonic generation in acoustic systems," Thesis, Harvard University, Cambridge, MA (1971).

[14]N. H. Fletcher, R. Perrin, and K. A. Legge, "Nonlinearity and chaos in acoustics," Acoust. Aust. **18**(1), 9–13 (1989).
[15]N. H. Fletcher, "Nonlinear dynamics and chaos in musical instruments," in *Complex Systems: From Biology to Computation*, edited by D. Green and T. Bossomaier (IOS Press, Amsterdam, 1993).
[16]C. Wilbur and T. D. Rossing, "Subharmonic generation in cymbals at large amplitudes," J. Acoust. Soc. Am. **101**(5), 3144 (1997).
[17]T. D. Rossing, "Acoustics of percussion instruments: Recent progress," Acoust. Sci. Technol. **22**(3), 177–188 (2001).
[18]A. Alippi, A. Bettucci, M. Germano, and D. Passeri, "Harmonic and subharmonic acoustic wave generation in finite structures," Ultrasonics **44**, e1313–e1318 (2006).
[19]J. Carson and T. Fry, "Variable frequency electric circuit theory with application to the theory of frequency modulation," Bell System Tech. J. **16**, 513–540, (1937).
[20]J. Ville, "Theorie et application de la notion de signal analytic,", Cables et Transmissions, Paris, France (1948), Vol. 2A(1), pp. 61–74 (translation by I. Selin, "Theory and applications of the notion of complex signal," Report No. T-92, RAND Corporation, Santa Monica, CA 1958).
[21]B. Boashash, "Estimating and interpreting the instantaneous frequency of a signal—Part 1: Fundamentals," Proc. IEEE **80**(4), 520–538 (1992).
[22]B. Boashash, "Estimating and interpreting the instantaneous frequency of a signal—Part 2: Algorithms and Applications," Proc. IEEE **80**(4), 540–568 (1992).
[23]H. Suzuki, F. Ma, H. Izumi, O. Yamazaki, S. Okawa and K. Kido, "Instantaneous frequencies of signals obtained by the analytic signal method," Acoust. Sci. Technol. **27**(3), 163–170 (2006).
[24]L. Rossi and G. Girolami, "Instantaneous frequency and short term Fourier transforms: Application to piano sounds," J. Acoust. Soc. Am. **110**(5), 2412–2420 (2001).